Packed-bed Thermocline Testing Facility with Air as HTF for Sensible Thermal Energy Storage

Elisa Alonso[1], Esther Rojas[1] and Rocío Bayón[1]

[1] Thermal Storage and Solar Fuels Unit, PSA-CIEMAT Madrid (Spain)

Abstract

Sensible heat from CSP plants or other energy sources can be stored in one-single tank storage system that performs by creating a thermocline between a cold and hot zone. The Thermal Storage Group of CIEMAT has available a testing facility for packed-bed thermocline TES, named ALTAYR, suitable for operating in a wide range of temperatures and flowrates, different solid materials and charge and discharge modes. Such facility is useful for forecasting the behavior of industrial thermocline tanks, especially when it is combined with mathematical models able to count for scale aspects, as well as for different material assessment. In this work, different experimental tests operating with ALTAYR under different conditions are presented. Two types of pebbles have been employed as filler materials and their storage capacity has been compared. The temperatures in both solid and air have been measured independently using four different experimental methodologies to differentiate between them. However, it appears to be no measurable difference. The tank wall thermal conductivity has been obtained from one long duration experimental test in order to characterize the tank and be able to calculate thermal losses through the wall.

Keywords: Thermal Energy Storage, Packed-bed Thermocline, Sensible Heat, CSP

1. Introduction

A CSP plant can include large thermal energy storage (TES), and thanks to it the electricity supply is possible for extended periods, even at night-time and it is not affected by short term variations due to clouds occurrence during the sunny time. This advantage over other renewable which does not count with storage of large capacity (wind and PV) provides high flexibility and dispatchability to CSP and makes it the key to have a renewable energy mix (Islam et al., 2018). Currently, the mainstream TES solutions are based on sensible heat storage (SHS) and use a molten salt mixture that are stored in a two tanks system, one tank devoted to hot salt and another to cold salt. However, compared to this system, an only one thermocline tank is about 35% cheaper (Gil et al., 2010). A thermocline tank usually contains a solid filler that occupy most of the total volume and, thus, contribute to reduce the global cost of the system. As fillers, cheap and locally available materials are normally employed. Natural materials such as sand or different kind of stones are common (Schlipf et al.,2014). They form a packed-bed through which a liquid or gas flows. This work focuses in an air-rock packed bed able to operate at maximum temperature over 700ºC. In a system of such characteristics and according to most of literature references, it is expected to find significant differences between air and solid temperature (Bayón and Rojas, 2013). Using the facility available at CIEMAT, named, ALTAYR, experimental methodologies have been devised and put in practice with the objective to differentially measure solid and air temperature. The general performance of the packed-bed tank has been also analyzed. The relevance of a deep understanding on this storage prototype behavior stands on the need of employing it as an experimental tool to: 1) study the effects of the main parameters which will be critical for an industrial-scale thermocline tank design, 2) validate numerical models developed to allow the analysis of a wide range of operation conditions, 3) study the goodness of different materials as storage media.

2. Experimental Facility

ALTAYR´s main component is a cylindrical tank with a bed height of 0.5 m (tank height 0.72 m) and 0.5 m in inner diameter. It consists of a metal casing with a ceramic inner wall, separated by an insultation layer. On and under the cylindrical main body there are two additional conical bodies coinciding with the air inlet and outlet. Working in charge mode, the hot air is heated by a set of electrical resistances. It flows to the tank thanks to a blower and a flowmeter -with a valve- that propel the atmospheric air toward the resistances container and

doi:10.18086/eurosun.2020.07.03 Available at http://proceedings.ises.org

following to the tank. Air temperature is set by using a control system configured in a control board. Temperature from ambient to more than 1000 ºC can be set and achieved by the resistances, although in this work the goal has been established in 700 ºC. The hot air crosses the tank from the top to the bottom and exists through the lower pipe, which, after a certain path, leads to outside.

The tank is provided with a fair number of thermocouples for temperature monitoring. In the rock-bed, temperature is measured at 9 different heights and 4 radiuses. Moreover, the temperature on the outer wall of the tank is measured at 10 heights and 5 angular positions and the air temperature at the inlet and outlet is also measured.

To modify the working mode to discharge, the pipes connections can be exchanged so that the tube coming from the blower would enter through the base of the tank and the hot air would exit through the top and would been ejected.

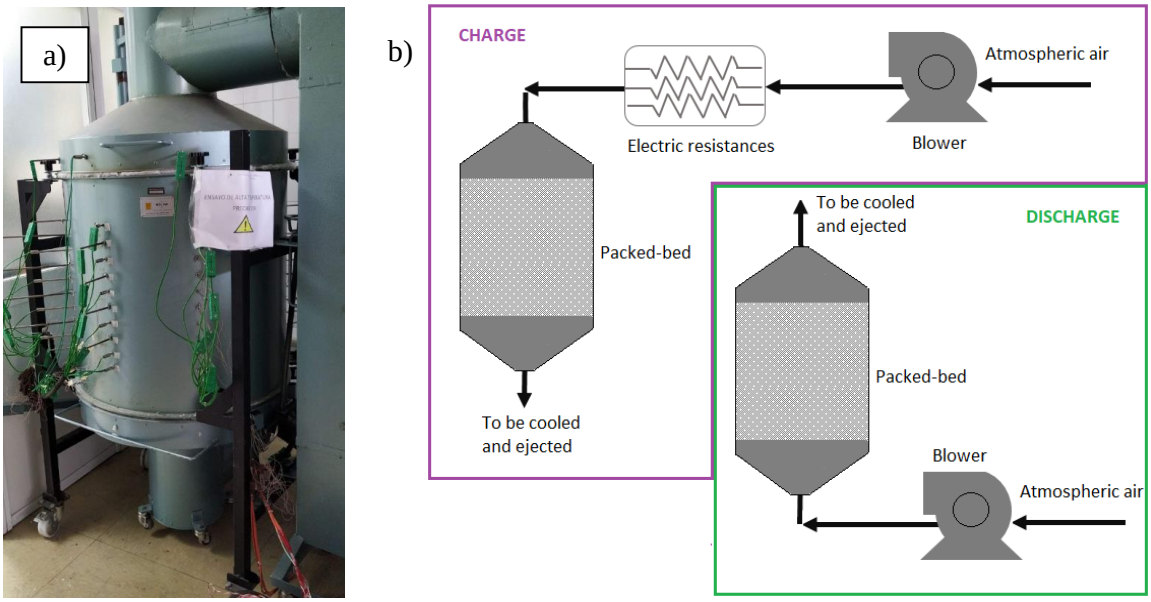

Fig. 1: a) Picture of ALTAYR packed-bed tank. b) Schematic of the main components of the experimental facility when working in charge and discharge modes.

3. Filler Characteristics

Two economic types of pebbles, easily reachable through gardening products suppliers, were purchased to be employed as filler materials. They are showed in Fig. 2 once they had been placed inside the tank. Composition of pebbles in filler 1 is not informed by the provider, who offer the material as “white boulder”. The mechanic resistance of the pebbles was noted to be low since they broke under light pressure. Filler 2 composition was specified by the provider as mainly SiO_2, with unknown purity. The porosity was obtained experimentally by measuring the water volume that fits on 0.1 m^2 of pebbles.

Tab. 1: Main properties of the two filler materials.

Property	Filler 1	Filler 2
Composition	Unknown	Mainly silica
Color	White	Beige
Size (mm)	12/25	14/22
Density (kg/m^3)	1790	1780
Porosity	0.37	0.31

Fig. 2: Two kind of fillers employed for the experimental tests.

4. Experimental tests

The tank was filled with around 150 kg of pebbles. Experimentation consisted in a set of tests of charge and discharge processes performed for each of the two filler materials. Threshold temperature during charge was stablished by setting up the air stream temperature in values between 300º C and 700 ºC. Discharge tests were started after ending charge and manually changing the tubing connections to lead the cold air at room temperature enter through the tank bottom. Air mass flowrates between 50 and 100 kg/h were employed for the different tests. The electric energy consumption to heat up the air was also accounted by means of a consumption meter. Figure 3 shows a detailed representation on the thermocouples position along the tank height and radius. Red and grey lines and dots correspond to thermocouples at alternate levels that are introduced inside the packed bed, touching the pebbles but completely surrounded by air. The temperature values they record are more likely the air temperature. Green lines and dots, instead, represent particular thermocouples that measure temperature inside the rocks for which one the following procedures has been applied:

- A: Taking a thermocouple provided with a rigid, metallic sheath, one of the stones was pierced to make a hole with around the same diameter than the sheath (6 mm) and about 5 mm in depth. The thermocouple was then inserted into the hole. This strategy was employed with filler 1 because filler 2 rocks could not be easily mechanized and broke when holes of 6 mm in diameter were tried.

- B: Taking a flexible, 0.5 mm in diameter thermocouple, it is inserted into a natural, small hole existing in a pebble. This strategy was employed with filler 2.

- C: A hole of around 3-4 mm in diameter was made in a stone. The hole was then filled with ceramic fiber and a flexible, 0.5 mm in diameter thermocouple was pricked. This strategy was employed with rocks of filler 2, which did not endure holes of 6 mm in diameter, but they did of smaller diameter.

- D: The front of a thermocouple provided with a rigid, metallic sheath was put in contact with a flat face of a stone. Avoiding the contact surface, the end of the thermocouple and the stone were covered by high temperature refractory cement that rapidly hardened.

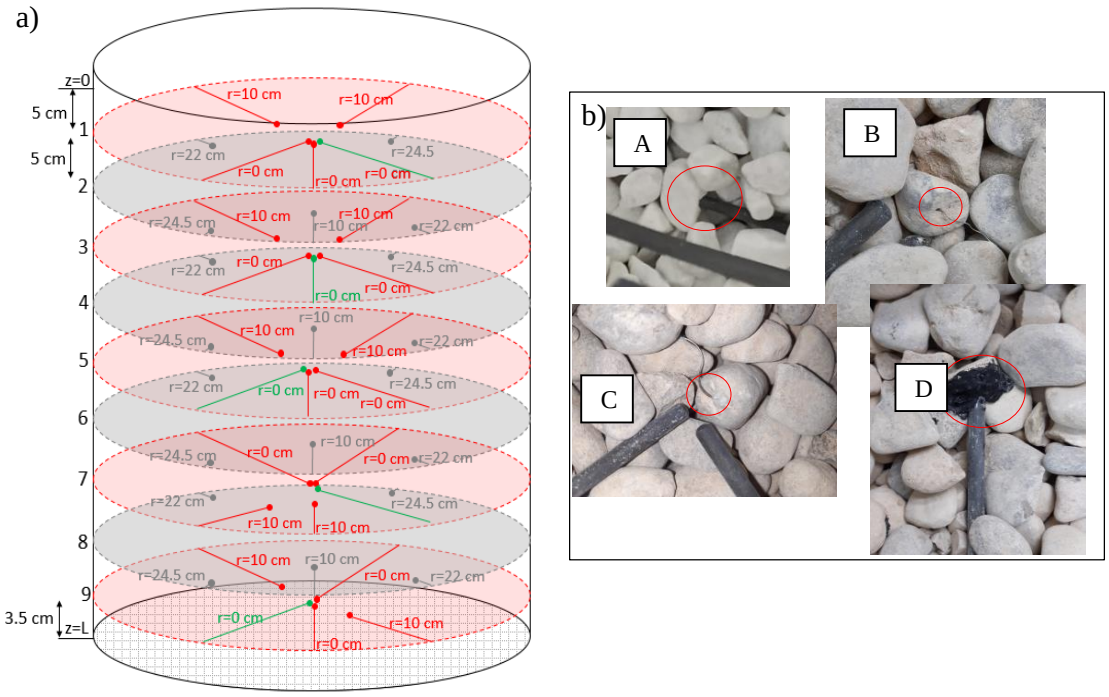

Fig. 3: a) Schematic of the thermocline tank where the positions of thermocouples have been indicated by height levels, radius and angles. b) Images of the thermocouples devoted to measure the solid temperature according to four different procedures described above.

5. Results

5.1. General performance

Figure 4 shows two experimental cases of charge performed for filler 1 (a and c) and discharge performed for filler 2 (b and d) using ALTAYR facility. For each one, data have been represented in both temperature versus time, as directly recorded by the data logger and temperature versus tank height to appreciate the time evolution of the thermocline.

Temperature data were recorded along the time as presented in Fig. 4 a) and c). Temperature curves correspond to thermocouples placed in the middle of the cylindrical tank, being the upper one that of maximum temperature and the lower one that of minimum. z values corresponding to the position of each thermocouple are 0, 0.05, 0.15, 0.25, 0.35 and 0.45 m. b) and d) correspond to the same cases but the thermocline formation along height is represented. During the experimental work, it was clearly observed that required time to charge and discharge is strongly influenced by the type of filler, the range of temperatures and the air mass flowrate. Next sections deepen in the effect of these parameters. The initial temperature of discharge case is not constant due to the facility requires manual actuation to change the working mode. That means that the experimenter employs a certain time to switch off the blower and the heater, to start a new data recording program and to change the position of two heavy tubes. The upper limit of the selected operation parameters range, that is, threshold temperature of 700ºC and flowrate of 100 kg/h were unsuccessfully achieved, because the heater needs to work at its limit of power and thus, reaching the temperature set point delays too much. Then, such a combination of parameters was avoided.

Charge data of temperature-time could be analyzed by fitting the experimental curves to an algebraic sigmoid function as previously reported in (Bayón and Rojas, 2018). For each tank position (zc), this curve fitting leads to a value of time (tc) that corresponds to the sigmoid inflection point. In this way, plotting zc vs. its corresponding tc it is obtained a linear variation whose slope is the thermocline velocity vTC. For the test of Figure 4 a) the thermocline velocity is $3.89 \cdot 10^{-5}$ m/s.

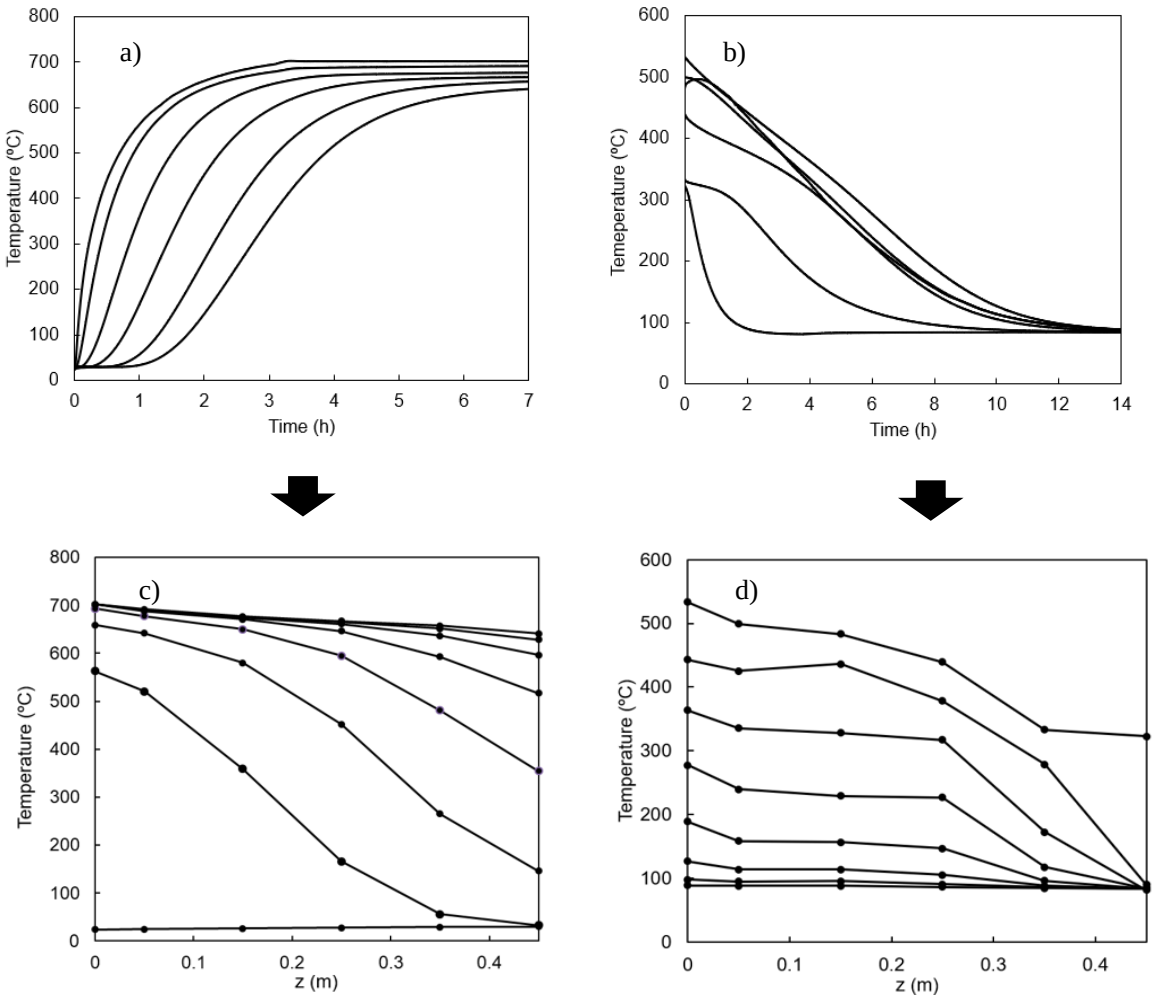

Fig. 4: Temperature distribution in two experimental case: a) and c): charge, maximum temperature 700 ºC, air flowrate 80 kg/h. b) and d)): discharge, maximum temperature 600 ºC, air flowrate 50 kg/h. Note that origin in z coordinate is considered in the top of the tank. The time gap between lines is 1 h for Fig. 4 c) and 2 h for Fig. 4 d), being the first one time equal to 0.

In energy storage systems, charge and discharge efficiencies are usually selected as performance indicators (Hoffmann et al., 2017). Their utility to assess the storage system is relevant when it is integrated in a plant that operates under determinate conditions to which the storage must be adapted. In those cases, the storage system performs charge and discharge cycles between two given threshold temperatures. Here, an instantaneous overall efficiency of the whole packed-bed facility has been calculated as the ratio between the stored energy and the supplied energy, which is globally accounted by the electricity consumption meter.

$$\eta_{overall} = \frac{m \cdot C_p (T_b - T_i)}{E_e} \qquad \text{(eq. 1)}$$

Figure 5 a) shows the overall facility efficiency evolution throughout a test with maximum temperature of 300ºC and a duration of 22 h. The packed-bed material was filler 2, mainly composed of silica, and which specific heat can be approximated to that of quartzite, that is, 840 J/kg·K (Gautan and Saini, 2020). Maximum efficiency takes place after around 6 hours of heating, being 6.8 %. The higher the maximum temperature, the higher the efficiency. For instance, in the case of the experiment represented in Fig. 9 (filler 2, 6 hours of heating with a threshold temperature of 700ºC) the maximum efficiency reaches 15.7% and takes place after 5.6 hours of heating (Figure 5 b)).

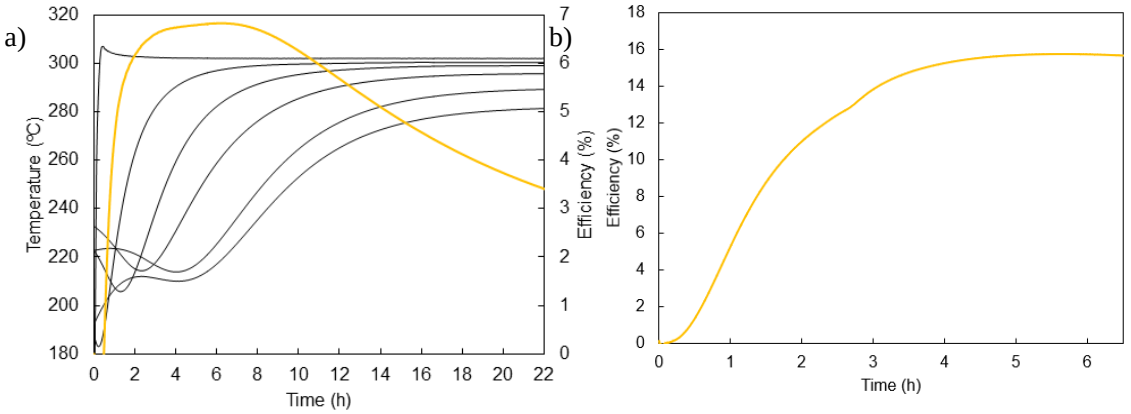

Fig. 5: Two examples of the overall facility efficiency. a) Test with filler 2, maximum temperature of 300ºC, duration of 22 h. Black lines show the temperature evolution in different tank heights (0, 0.05, 0.15, 0.25, 0.35 and 0.45) b) Test with filler 2, maximum temperature of 700ºC, duration of 6 h. Figure 4 b) corresponds to the temperature evolution represented by red curves in Fig. 9.

5.2. Solid and air temperature

The temperature differences between solid and air is not high enough to be evaluated by means of any of the measurement strategies applied in this work. In Fig.6 four examples of comparison of solid and air temperatures are showed. Each one of the described methods have been employed to difference them, which have been measured at the same height and radius. As observed, the differences between solid and air temperature is not higher than the own error between the two measurements of air temperature taken by two equal thermocouples placed together.

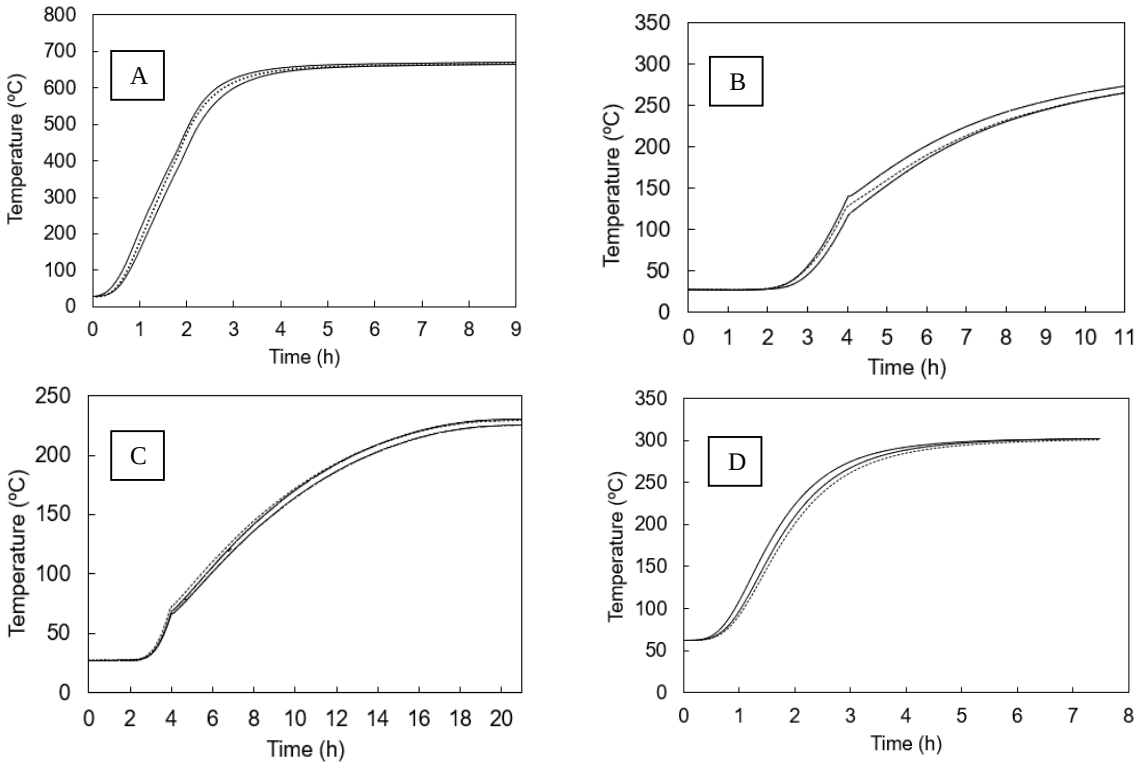

Fig. 5: A result example of each strategy to differentiate solid temperature from air one. Each letter corresponds to the case indicated in section 4.

5.3. Air mass flowrate influence in the thermocline behaviour

It is expected the air flowrate introduced in the tank, which directly affects the interstitial air velocity, modifies the velocity of the thermocline. Figure 7 is devoted to show this effect. The thermoclines of four experimental cases, which operation conditions are indicated in Tab. 2, are represented for 8 hours of charge and temporal gaps of 1 hour. 8 hours is enough time to completely charge the tank when the maximum temperature is 300 in both cases although the charge is faster for a flowrate of 100 kg/h. In this case, the tank is also practically charged after 7 hours. When the maximum temperature is higher, as observed in cases A and B, the required time to charge de tank is obviously higher as well. However, comparing cases A and B it is clearly observed how the higher the air flowrate, the faster the progression of the thermocline. More than visually, the thermocline behaviour can be compared with accuracy by calculating the vTC according to Bayón and Rojas, 2018, and as explained above. The corresponding values have been included for each case in the last column of Tab. 2.

Tab.2. Operational conditions of the cases showed in Fig. 6.

Case	Filler	T_{max} (ºC)	Air flowrate (kg/h)	vTC (m/s)
A	1	700	50	$3.15 \cdot 10^{-5}$
B	1	700	80	$3.89 \cdot 10^{-5}$
C	1	300	80	$7.41 \cdot 10^{-5}$
D	1	300	100	$8.09 \cdot 10^{-5}$

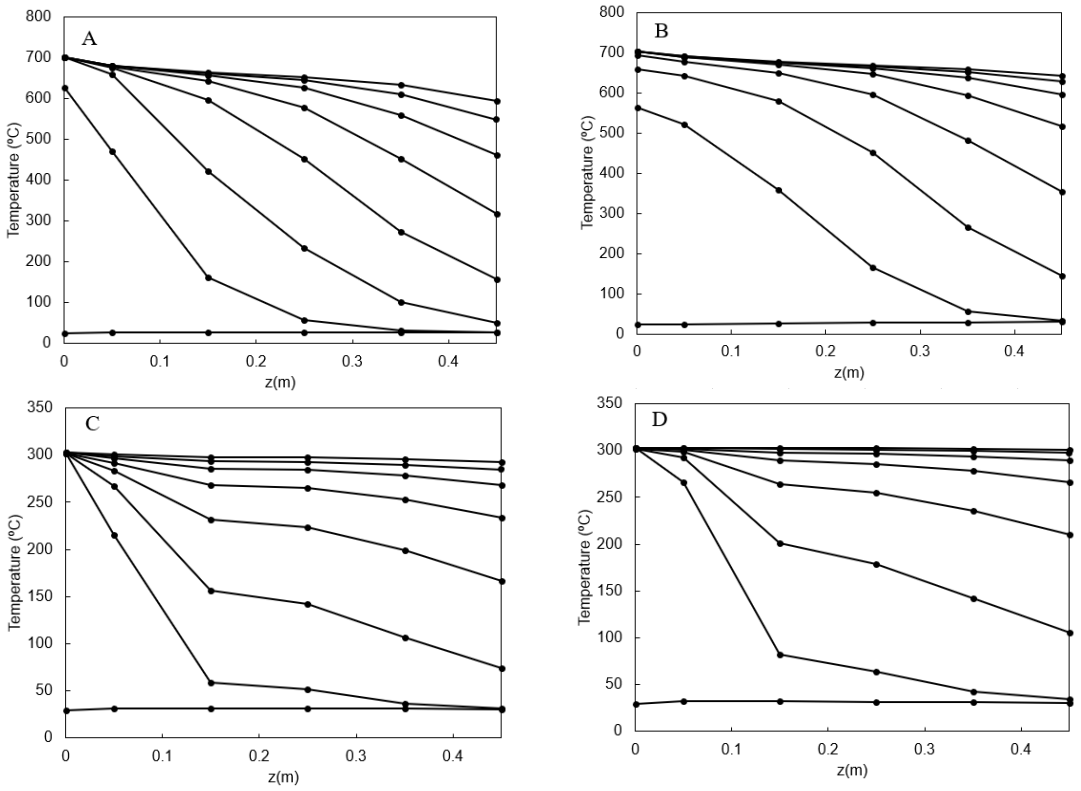

Fig. 7: Thermocline formation and evolution for maximum temperature 700 ºC and 2 values of air flow mass and for maximum temperature 300 ºC and 2 values of air flow mass (see Tab. 2) . The time gap between lines is 1 h, being the first one time equal to 0.

5.4. Wall heat transfer coefficient

The experimental case reported in Fig. 4 a) was retained to calculate global heat transfer coefficient through the tank wall. In that experiment, due to its long duration, stationary thermal conditions were achieved both in the packed-bed and the external wall (see Fig. 8). Known the air flowrate and the values of temperature, an energy balance applied to the tank can be expressed as follows:

$$\dot{m_{air}} Cp_{air}(T_{in} - T_{out}) = \frac{2\pi k_{wall} L(T_{wall,int} - T_{wall,ext})}{ln\frac{r_{ext}}{r_{int}}} \qquad \text{(eq. 2)}$$

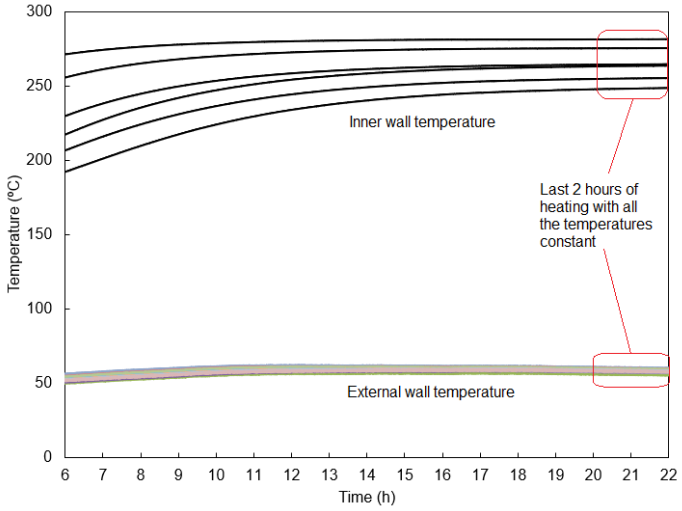

Fig. 8: Experimental case with maximum temperature 300 ºC and 50 kg/h of air flowrate used to calculate the global heat transfer coefficient of the tank wall. The figure focuses on the region where temperatures

According to eq. 2 k_{wall}, which corresponds to the global conductivity involving all the wall layers is 0.4 W/m·K.

Once known k_{wall}, thermal losses can be calculated during the experiments. For comparative purposes, three different cases have been represented. Table 3 shows the operational conditions of each one.

Tab.3. Operational conditions of the cases showed in Fig. 8.

Case	Filler	T_{max} (ºC)	Air flowrate (kg/h)
A (blue)	1	700	50
B (yellow)	2	300	50
C (green)	2	300	100

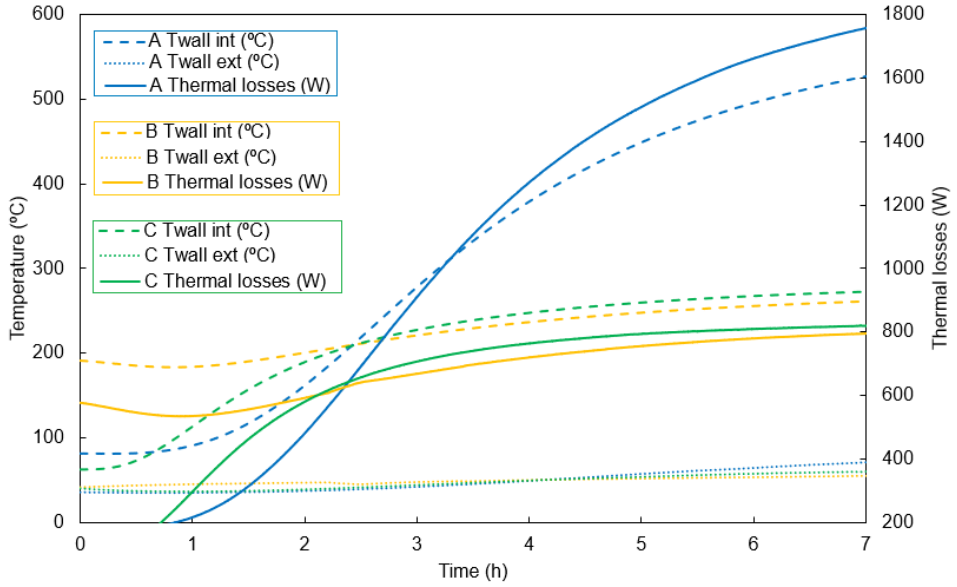

Fig. 9: Inner wall and external wall temperatures and thermal losses through the tank wall calculated for three different experimental cases defined in Tab. 3.

Moreover, known the electric consumption to heat up the air, and neglecting the losses to convert electricity into heat, the thermal losses in the heater and along the tube from heater to tank are also calculated, which, for this experimental test, results of 174.8 W.

5.5. Comparison between the two fillers

By comparing two tests under similar operational conditions, each one using one type of filler, the first observed result is the higher storage capacity of filler 2, probably due to its higher specific heat. They are represented in Fig.10. Both tests consumed 78±2 kWh_e for 6 hours of heating, with a T_{in} set in 700 ºC and a flowrate of 50 kg/h. As observed in Figure 9 filler 1, represented in green, achieved much higher average temperature than filler 2, in red. Thermal losses thorough the tank wall are lower in the case of filler 2. In other words, the total thermal capacity of the storage system with filler 1 is much closer to be completed than with filler 2 after 6 hours of heating. Ensayed et al. (1988) defined the Bed Storage Factor (BSF) as the ratio of energy stored in the bed at a moment of time to the maximum possible energy storage in the bed:

$$BSF = \frac{m \cdot C_p (T_b - T_i)}{m \cdot C_p (T_{max} - T_i)} \qquad \text{(eq. 3)}$$

where T_{max} is the maximum temperature of air inlet, T_i is the initial temperature of the bed and T_b is the average bed temperature achieved in the considered time. Such a definition is equivalent to the capacity ratio found in (Hänchen et al. ,2011). Since thermocouples placed in the packed bed are equidistant, T_b can be calculated as the direct average temperature of the 5 measured values after 6 hours, excluding T1 that corresponds to the air inlet temperature and it is taken above the packed-bed in the air stream. T6 is taken inside the bed at its bottom, but the values are so close to the air outlet temperature that both curves overlap in Fig. 9. T2 to T6 are the values measured by the thermocouples distributed downstream in the tank. According to Eq. 3 BSF is 0.89 for filler 1 and 0.49 for filler 2. Neglecting differences in thermal losses for rapid estimation purposes, the total storage capacity is around 1.8 times higher with filler 2, as schematically represented by the blue rectangles in Fig. 9. The whole rectangles would represent the total capacity for each case and the blue area would correspond to the full fraction after 6 hours according to the graphed experiments. vTC for both cases have been also calculated and their values are $3.145 \cdot 10^{-5}$ m/s for filler 1 and $3.097 \cdot 10^{-5}$ m/s for filler 2.

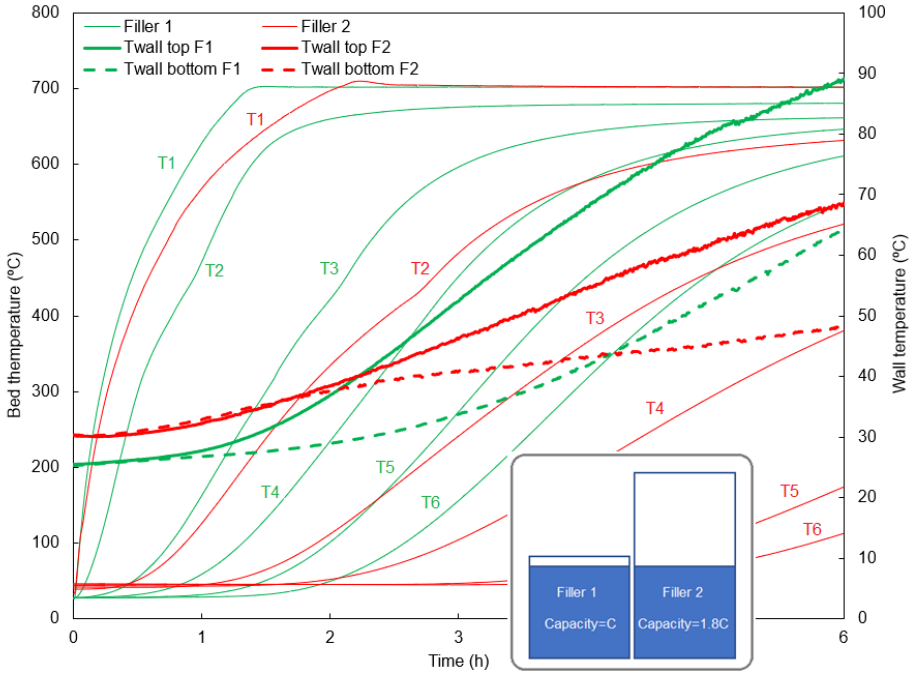

Fig. 10: Comparison between the performance of the storage system using two types of fillers. Charging tests with mass flowrate 50 kg/h and maximum temperature 700 ºC.

Considering a constant C_p of filler 2 of 840 J/kgK (as reported in Gautan and Saini, 2020 for quartzite), the maximum theoretical storage capacity of the system containing filler 2 would be 84 MJ and containing filler 1 47 MJ.

6. Conclusions

ALTAYR tank protype was assessed as a tool for air-solid thermocline studies. Two different filler materials were tested and the second one, which composition is basically SiO_2, presented storage capacity around 1.8 times the first tested material. The tank is useful to measure thermocline velocities under different working conditions, as it is able to operate in a large range of temperature and air flowrates. It was probed how thermocline velocity increases with air flowrate and decreases with maximum set temperature in charge experiments. The global conductivity of the tank wall, including all the layers, was calculated by means of a steady state experiment in which inner and external wall temperature maintained constant. Its value is 0.4 W/m·K. Four strategies to discriminate solid and air temperature were tried. However, the temperature differences between solid and air was not high enough to be evaluated by means of any of the measurement methods applied in this work. Instead, the differences between solid and air temperature was not higher than the own experimental error.

7. Acknowledgments

The authors wish to thank "Comunidad de Madrid" for its support to the ACES2030-CM project (S2018/EMT-4319) through the Program of R&D activities between research groups in Technologies 2018, co-financed by European Structural Funds.

8. References

Bayón, R., Rojas, E. 2013. Simulation of thermocline storage for solar thermal power plants: From dimensionless results to prototypes and real-size tanks. Int. J. Heat Mass Transf. 60, 713–721.

Bayón, R., Rojas, E. 2018. Analysis of packed-bed thermocline storage tank performance by means of a new analytical function. AIP Conf. Proc. 2033, 090002.

Elsayed, M.M., Megahed, I.E., El-Refaee, M. M. 1988. Experimental testing of fluidized bed thermal storage. Sol. Wind Tech. 5, 15–25.

Gautam, A., Saini, R.P. 2020. A review on sensible heat based packed bed solar thermal energy storage system for low temperature applications. Sol. Energy. 207, 937–956.

Gil A., Medrano M., Martorell I., Lázaro A., Dolado, P., Zalba B., Cabeza L. 2010. State of the art on high temperature thermal energy storage for power generation. Part 1—Concepts, materials and modellization. Renew. Sustain. Energy Rev. 14, 31–55. Ç

Hänchen, M., Brückner, S., Steinfeld, A. 2010. High-temperature thermal storage using a packed bed of rocks-Heat transfer analysis and experimental validation. App. Th. Eng. 31, 1798–1806.

Hoffmann, J. F., Fasquelle, T., Goetz, V., Py, X. 2017. Experimental and numerical investigation of a thermocline thermal energy storage tank. App. Th. Eng. 114, 896–904.

Islam M.T., Huda N., Abdullah A.B, Saidur R. 2018. A comprehensive review of state-of-the-art concentrating solar power (CSP) technologies: Current status and research trends. Renew. Sustain. Energy Rev. 91, 987–1018.

Schlipf, D., Schicktanz, P., Maier, H, Schneider, G. 2015.Using sand and other small grained materials as heat storage medium in a packed bed HTTESS. Energy Procedia. 69, 1029–1038.